Crystallization of Poly(L-lactic acid) Probed with Dielectric Relaxation Spectroscopy

Ana Rita Brás,[†] María Teresa Viciosa,[†] Yaming Wang,[‡,§] Madalena Dionísio,[†] and João F. Mano*[,‡,§]

REQUIMTE/CQFB, Departamento de Química, FCT, Universidade Nova de Lisboa, 2829-516 Caparica, Portugal; 3B's Research Group-Biomaterials, Biodegradables, Biomimetics, Department of Polymer Engineering, University of Minho, Campus de Gualtar 4710-053 Braga, Portugal; and Department of Polymer Engineering, University of Minho, Campus de Azurém 4800-058 Guimarães, Portugal

Received May 22, 2006; Revised Manuscript Received July 14, 2006

ABSTRACT: The properties of the amorphous component in poly(L-lactic acid), PLLA, depend on its crystalline structure, where the nanoconfinement effects may be monitored using dielectric relaxation spectroscopy. In this work this technique is used to monitor isothermal crystallization in PLLA by probing the evolution of the loss peak with crystallization time. It was found, for two different molecular weight materials and by crystallization from either the glassy or melt states, that the data could be given by a linear combination of three loss processes, where just their intensities vary: the α-process of the amorphous material, the constrained α-process present in the fully crystallized material, corresponding to the segmental motions of the amorphous phase confined by the crystalline lamellae, and the sub-glass β-relaxation. The appearance of the confined process was detected in the earlier stages of the crystallization, suggesting that the confinement effects are effective during primary crystallization. In this case, the cooperative segmental motions are restricted by the primary lamellae, leading to a dynamics characterized by a broader relaxation time distribution shifted to higher values. It was observed that the crystallization, as investigated by monitoring the evolution of the amorphous phase, is quicker for lower molecular weight PLLA and is slower for the material crystallized from the melt with respect to the cold crystallization. It was found that the confined dynamics is not very dependent on the thermal history prior to the crystallization step. The features of the β-relaxation were found to be similar for amorphous and semicrystalline systems, indicating that the sub-glass process in PLLA is not influenced by the crystalline confinement.

1. Introduction

Poly(L-lactic acid), PLLA, is a well-studied biodegradable and biocompatible linear aliphatic polyester due to its applicability in different fields, such as biomedical applications,[1−4] including in wound closures, prosthetic implants, controlled delivery systems, and three-dimensional porous scaffolds for tissue engineering, as well as in environmental applications. Biodegradation is a key factor in such applications, and PLLA may degrade in natural environments, leading to monomers and oligomers that can be metabolized by various microorganisms.[2] Moreover, a series of aspects make this material also interesting to be studied in a more fundamental point of view. This includes the fact that PLLA crystallizes slowly,[5−7] which allows preparing materials with tuned degrees of crystallinity and lamellar morphologies, by changing the thermal history. In this context, crystallinity will also be important in the application point of view as it will influence the degradation profile,[8] the mechanical properties,[9] and even the cell response to PLLA substrates.[10]

The crystallization process in polymers has been traditionally performed by monitoring the evolution of the development of the crystalline structure at different length scales, using techniques such as atomic force microscopy, transmission electronic microscopy, small- and wide-angle X-ray scattering, small-angle light scattering, or differential scanning calorimetry (DSC). Such data can be complemented by looking at the changes occurring within the amorphous fraction upon crystalline development. Such information may be instructive as the amorphous regions will play an important role in the properties of the material, in particular in systems that not crystallize up to very high contents, such as in PLLA. Moreover, the glass transition of PLLA is not far above room or body temperature; therefore, it expected that, due to the presence of an amorphous phase, the physical properties of the material will change with time due to structural relaxation, such as the changes found in the mechanical behavior.[11]

Therefore, it is important to understand how the amorphous regions coexist with the crystalline phase. It is well-known that in semicrystalline polymers the amorphous regions will be placed within the spherulitic structures and confined between the crystalline lamellae or lamellae stacks.[12] When confined in geometry with length scales of some nanometers, polymeric chains exhibits a conformational dynamics different from the bulk.[13] The effect of the confinement in the glassy dynamics is still controversial, despite the great amount of experimental and theoretical results,[14] and more insights into other systems are still needed. Therefore, semicrystalline polymers may also constitute a valuable model to study the dynamic behavior of polymeric chains in nanoconfined conditions.[15]

Dielectric relaxation spectroscopy (DRS) is an adequate technique to investigate the chain dynamics of polymers.[16] The evolution of the dielectric α-relaxation, associated with the dipolar fluctuations resulting from segmental motions along the chain backbone, has been used as a probe for the change in the glass transition dynamics upon crystallization, including in PLLA.[17−19] Some contradictory results were found, for example,

* Author for correspondence. E-mail: jmano@dep.uminho.pt.
[†] Universidade Nova de Lisboa.
[‡] 3B's Research Group-Biomaterials, Biodegradables, Biomimetics, University of Minho.
[§] Department of Polymer Engineering, University of Minho.

10.1021/ma061148r CCC: $33.50
Published on Web 08/18/2006

in the shifting of the position of the loss peak: Mijović and Sy did not observed any change in the loss peak position during crystallization of PLLA at 80 °C;[17] Fitz and Andjelić observed a shift to higher frequencies in PLLA at similar conditions, but the crystallization was performed in partial constrained conditions, i.e., the volumetric contraction that occurs during solidification was avoided.[18] In a previous work we observed a consistent shift to lower frequencies.[19]

It is also far to be understood the attribution of the changes occurring in the glass transition dynamics during crystalline development. In fact, as discussed by Lee et al., is it even still controversial the structural changes occurring in the organization of the crystalline fraction, especially during secondary crystallization.[20] In a previous work, it was observed, on the basis of both DSC and morphological data, that during crystallization at least two independent glass transitions could be found.[21] The lower glass transition temperature process (bulk glass transition), which decreases in intensity during crystallization, should be assigned to the conformational mobility within the bulklike amorphous phase, essentially present in the interspherulitic spaces. In fact, this process is absent when the spherulites finish by occupying all the available volume of the sample. A higher glass transition temperature process (glass transition of the semicrystalline material) should occur in an amorphous fraction in which the segmental motions are influenced by the confinement effect produced by the crystalline environment. It was suggested that this constrained amorphous phase could be located between the crystalline lamellae. The existence of the two independent processes was confirmed by DRS measurements performed during crystallization of a PLLA at 80 °C.[19]

In this work, we pretend to provide further information concerning the evolution of the glass transition dynamics upon crystallization. In particular, two PLLA with different molecular weights will be compared. Moreover, crystallization occurring at the same temperature but initialized from both the glassy and melt stages will be also confronted. In fact, it is known that, at least in terms of nucleation, the two thermal histories lead to completely different crystalline morphologies at the spherulitic length scales. It would be interesting to check whether this would influence the dynamics of the confined amorphous phase. To elucidate further such effect, DRS will be performed on fully crystallized materials, covering both the α-relaxation and the secondary process (β-relaxation).

2. Experimental Section

The material studied in this work is from Purac Biochem with an inherent viscositiy of 5.87 dL/g. The molecular weights, M_n and M_w, of the polymer, evaluated from gel permeation chromatography (Shimadzu, LC 10A, Japan) using polystyrene as standard and chloroform as solvent, are 269 000 and 301 000, respectively; thus, this sample is designated as $PLLA_{269kD}$. A $PLLA_{269kD}$ film was prepared by melting the material in a hot plate (at ca. 200 °C), compressed between two metallic disks, and quenching it in cold water. The PLLA film obtained is amorphous as checked by DSC and X-ray diffraction. The sample was then evacuated at about 50 °C for 48 h to remove absorbed water. The cooling to room temperature was accomplished under vacuum. After that, the $PLLA_{269kD}$ film was placed between two gold-plated electrodes (diameter 10 mm) of a parallel-plate capacitor for dielectric measurements that were carried out using a broadband impedance analyzer, Alpha-N from Novocontrol GmbH. The sample cell (BDS 1200) was mounted on a cryostat (BDS 1100) and exposed to a heated gas stream being evaporated from a liquid nitrogen dewar. The temperature control was performed within ±0.5 °C with the Quatro Cryosystem. Novocontrol GmbH supplied all these modules.

Before inducing crystallization, the amorphous sample was cooled to −120 °C and dielectric spectra were collected in increasing temperature steps from −120 up to 25 °C: in the temperature range −105 °C ≤ T ≤ −70 °C the dielectric spectra were recorded every 2 °C; in the remaining temperature region the spectra were recorded every 5 °C.

Scheme 1. Experimental Procedure Illustrating How Isothermal Spectra Were Collected

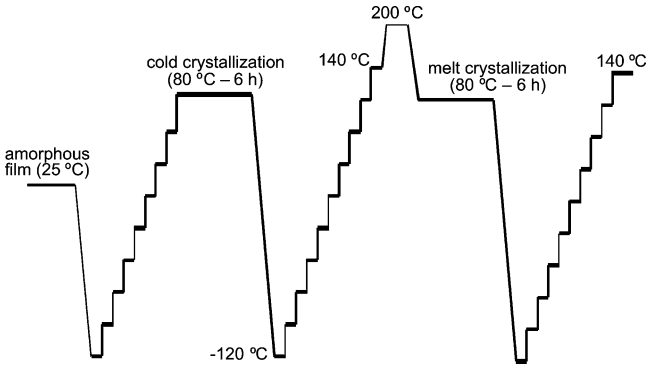

After this procedure dielectric spectra were acquired, isothermally (T = 80 °C) every 2 min, for 6 h; the crystallization achieved in these conditions will be designated as *cold crystallization*. Next the sample was cooled to −120 °C, and the dielectric spectra were collected up to 140 °C; in the temperature range −105 °C ≤ T ≤ −70 °C and 60 °C ≤ T ≤ 100 °C, the dielectric spectra were recorded every 2 °C; in the remaining temperature region the spectra were recorded every 5 °C.

Then the sample was heated to 200 °C and kept 2 min at that temperature to ensure melting and immediately cooled to 80 °C. At this temperature, the crystallization was monitored according to the same procedure followed during cold crystallization; the crystallization achieved in these conditions will be designated as *melt crystallization*.

Finally, the sample was refrigerated to −120 °C, and dielectric spectra were collected in increasing steps from −120 up to 140 °C, according to the same preset as followed after the cold crystallization procedure. Scheme 1 illustrates this experimental procedure.

During both types of crystallization, the real and imaginary parts of the complex permittivity were measured at 23 frequency values within the range from 100 Hz to 1 MHz, in such a way that each spectrum was collected in a time that does not exceed 1 min. This warranted that during any frequency scan the change in crystallinity was significantly small. In the remaining experiments data were acquired in an enlarged frequency range, from 1 Hz to 1 MHz in a total of 48 frequency values.

Additional differential scanning calorimetry (DSC) measurements were carried out in a Setaram DSC 131 using nitrogen as a purge gas. The temperature and heat of transition of the instrument were calibrated with indium at 10 °C/min. The weight of the sample was about 10 mg, which was cut from the amorphous film. To get the glass transition temperature of the amorphous $PLLA_{269kD}$, the heat flow of the amorphous sample was recorded during heating from 27 to 80 °C at 10 °C/min. Next the sample was kept at 80 °C for 8 h to obtain well cold-crystallized sample, then the sample was quenched to 27 °C, and the heat flow of the sample was recorded during heating from 27 to 200 °C at 10 °C/min. The sample was kept at 200 °C for 2 min and immediately cooled to 80 °C and kept at this temperature for 8 h to obtained well melt-crystallized sample. Then the sample was quenched to 27 °C, and the heat flow of the sample was recorded during heating from 27 to 200 °C at 10 °C/min. The glass transition temperature was taken as the midpoint of the transition.

3. Results and Discussion

3.1. Amorphous State. The $PLLA_{269kD}$ glass transition temperature observed by DSC was 60.8 °C. Therefore, we estimate that the α-relaxation in the amorphous state it is only

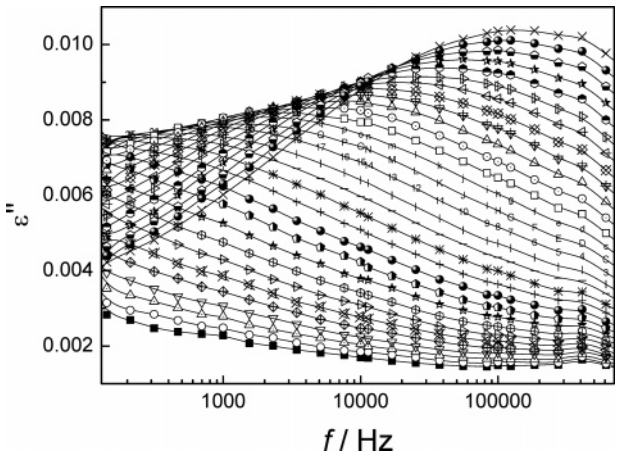

Figure 1. Dielectric loss spectra of the secondary relaxation process detected in amorphous $PLLA_{269kD}$, within the temperature range from −120 to 25 °C, in steps of 5 °C.

observable in our frequency window above 68 °C, which means that its characterization would imply to scan temperatures that crossed the crystallization onset, $T \geq 80$ °C. Consequently, data acquisition would be only possible in a quite narrow temperature interval. Therefore, the α-process in the amorphous state was not characterized (moreover, some DRS results on amorphous PLLA were already reported before[17,22]). Thus, before crystallization, the PLLA samples was only measured from −120 up to 25 °C (see Experimental Section) to characterize the β secondary relaxation, whose dielectric loss spectra are shown in Figure 1.

The loss curves of the β secondary process were fitted by the well-known Havriliak−Negami (HN) function:[23]

$$\epsilon^*(\omega) = \epsilon_\infty + \frac{\Delta\epsilon}{[1 + (i\omega\tau)^{\alpha}]^{\beta}} \quad (1)$$

where $\Delta\epsilon = \epsilon_s - \epsilon_\infty$ is the dielectric strength, i.e., the difference between the real permittivity values at respectively the low- and high-frequency limits, $\tau \approx (2\pi f_{max})^{-1}$ is the characteristic relaxation time, and α_{HN} and β_{HN} are the shape parameters ($0 < \alpha_{HN} < 1$, $0 < \alpha_{HN}\beta_{HN} < 1$); the α_{HN} value is related to the broadness of the relaxation while β_{HN} describes its asymmetry (Debye behavior is given by $\alpha_{HN} = \alpha_{HN}\beta_{HN} = 1$).

For the β-relaxation detected in the amorphous state, the α_{HN} and β_{HN} shape parameters were found to be 0.28 ± 0.02 and 0.79 ± 0.03, respectively. The linear temperature dependence of the relaxation time, shown later on, originates an activation energy of 50 kJ mol^{-1}. The low value of α_{HN} indicates that the β-relaxation is characterized by a broad distribution of relaxation times, typically attributed by the existence of a large variety of environments felts by the relaxing species.[16] Because of the inexistence of polar side groups in the PLLA chain, this secondary process has been assigned to twisting motions in the main chain. Combining dielectric and dipolar moment calculations, Ren et al. estimated that the amplitude of such motions in poly(DL-lactic acid) could be described by an average twisting angle of around 11°.[24]

3.2. Isothermal Crystallization at 80 °C. The $PLLA_{269kD}$ sample was afterward heated to 80 °C, and isothermal loss spectra were collected for 6 h (*cold crystallization* process). Figure 2a presents the dielectric loss curves each 10 min for the first 4 h; the last two curves were collected after respectively 5 and 6 h.

Besides the expected decrease in the intensity, the main loss peak shifts continuously toward lower frequencies almost 1 decade. A similar trend was obtained from melt crystallization at 80 °C with a lower molecular weight PLLA ($M_n = 86\,000$, $M_w = 151\,000$) reported in ref 19, here designated as $PLLA_{86kD}$. In that case, the dielectric loss curves were able to be fitted as a sum of three relaxation processes: (i) the β secondary process in the high-frequency flank, (ii) an α-process of the bulklike (nonrestricted) amorphous phase, similar to the one found in nearly amorphous material (α_{NA}), and (iii) an α-process of the amorphous fraction influenced by the crystalline structure, similar to the one found in fully transformed material (α_{SC}).

The rational behind this strategy is that previous DSC data of PLLA with increasing crystallinity degree exhibited two glass transitions where the intensity of the lower temperature one (bulklike process) decreased and the intensity of the higher temperature process, assigned to the constrained segmental mobility, increased.[21] Moreover, as the positions in the temperature axis of the two processes were essentially constant, we may hypothesize that during crystallization the characteristic times of the two processes could be unchanged. Therefore, as preliminarily tested in the previous work,[19] we tried to fit the data obtained with the $PLLA_{269kD}$ film during melt crystallization at 80 °C by keeping constant the shape parameters and relaxation time, just with their dielectric strengths varying; thus, instead of altering 12 parameters as will be the case if we assumed in the fitting procedure three arbitrary relaxation functions, only three parameters, $\Delta\epsilon$ of each HN relaxation function, were allowed to change. Therefore, we hypothesize that the global loss peak could be given by a simple linear combination of the intensities of the pure loss peaks of the three relaxation processes:

$$\epsilon''(t_c,\omega) = \Delta\epsilon_{\alpha_{NA}}(t_c)\,\epsilon''_{\alpha_{NA}}(\omega) + \Delta\epsilon_{\alpha_{SC}}(t_c)\,\epsilon''_{\alpha_{SC}}(\omega) + \Delta\epsilon_{\beta}(t_c)\,\epsilon''_{\beta}(\omega) \quad (2)$$

where $\epsilon''_{\alpha_{NA}}$, $\epsilon''_{\alpha_{SC}}$, and ϵ''_{β} are the normalized loss peaks of the pure α_{NA} (from the results at $t_c = 0$), pure α_{SC} (obtained from the results after maximum crystallization, at $t_c = 6$ h), and β. For the case of the β-relaxation, the loss peak features were obtained from the fitting of the initial or final data that essentially lead to the same shape parameters. In all cases, the loss peaks of the pure processes were assumed to behave as HN functions (eq 1).

The solid lines in Figure 2a correspond to the overall fitting assuming eq 2. The inset shows the loss spectrum obtained after 160 min, the obtained fit, and the corresponding three individual HN functions; superimposed is the real permittivity where the solid line is the fitting obtained using the same three HN functions, confirming the applicability of the Kramers−Kronig relations. The parameters used to fit both α-relaxations were the same found to fit the loss data of $PLLA_{86kD}$, i.e: for the α_{NA} loss peak the α shape parameter (α_{HN}) and relaxation time (τ) were 0.53 and 4.80×10^{-5} s, respectively, whereas for the α_{SC} loss peak the corresponding α_{HN} and τ values were 0.43 and 5.06×10^{-4} s; both β shape parameters (β_{HN}) were found to be unit. The β-relaxation was fitted with $\alpha_{HN} = 0.38$ and $\beta_{HN} = 0.82$, as for $PLLA_{86kD}$, but a slightly different relaxation time was used, 1.4×10^{-7} s, obtained by the extrapolation of the activation plot of the secondary relaxation process detectable at lower temperatures.

As found in most polymeric systems, the α_{SC} loss peak is typically shifted toward lower frequencies with respect to the nearly amorphous material.[16] It should be noticed that one may have an opposite behavior in some confined systems, where cooperative motions in geometrical constrained regions can be

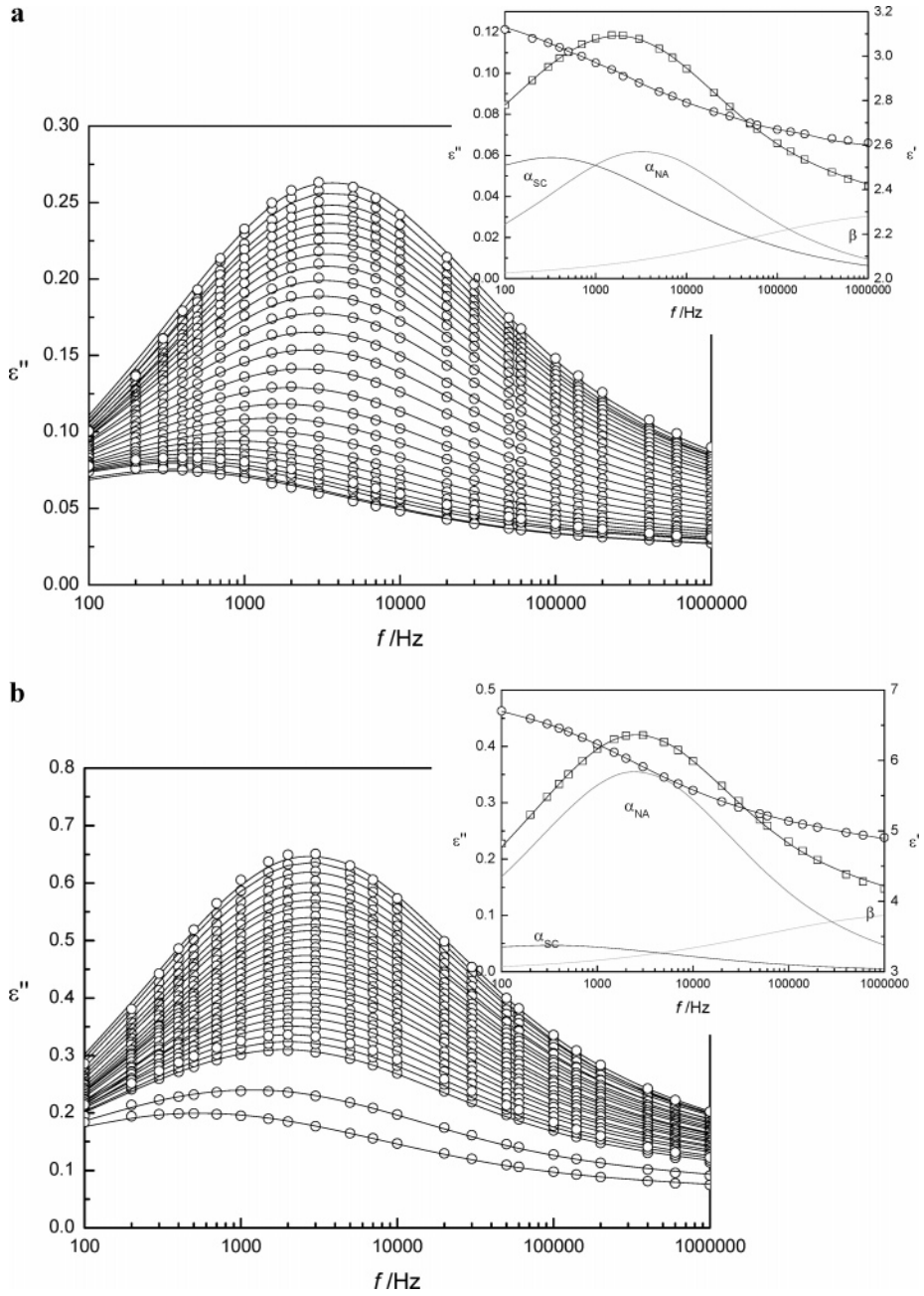

Figure 2. Dielectric loss spectra (circles) at 80 °C for $PLLA_{269kD}$ during **(**a) cold crystallization and (b) melt crystallization. The solid lines are the fitting obtained using the sum of three Havriliak−Negami (HN) functions (see eq 2). Only the loss curves collected each 10 min are shown for the first 4 h, and the last two curves were collected at respectively 5 and 6 h. The inset graphics shows the experimental results at 160 min for the imaginary (squares) and real (circles) parts of the complex permittivity fitted by taking into account three HN individual curves (solid lines).

faster than in the bulk (e.g., refs 25 and 26). Such behavior exists in systems where the geometrical confinement is dominant with respect to interactions existing between the relaxing groups and the nanoreservoir walls. In the case of the system studied in this work, there is a clear geometrical confinement: in a previous study, where PLLA was crystallized at different temperatures both from the melt and glassy states, X-ray scattering and DSC results allowed to estimate that the mobile amorphous layer exhibited thicknesses between 6 and 8 nm, confined between rigid amorphous layers with thicknesses of 2−4 nm and crystalline layers with 13−26 nm thicknesses.[27] When surface interactions are present the relaxation time slows down, resulting in a loss peak at lower frequencies or a higher T_g. This behavior is effectively present in semicrystalline polymers were the chains in the mobile amorphous layer are tightly linked to the rigid amorphous layer through covalent bonds.

The evolution of the dielectric strength upon cold crystallization of $PLLA_{269kD}$ is presented in Figure 3 (squares), for the nearly amorphous (top) and semicrystalline (middle) α-relaxations and for the *β*-process (bottom). The data were normalized by the maximum value obtained for the nearly amorphous α-process for comparison purposes.

The maximum transformation degree was reached after 200 min with the dielectric strength of the bulklike relaxation process becoming null and the constrained glass transition relaxation process attaining a steady value.

As described in the Experimental Section, the same sample of $PLLA_{269kD}$ was further crystallized isothermally at 80 °C after melting at 200 °C (melt crystallization process). Dielectric loss

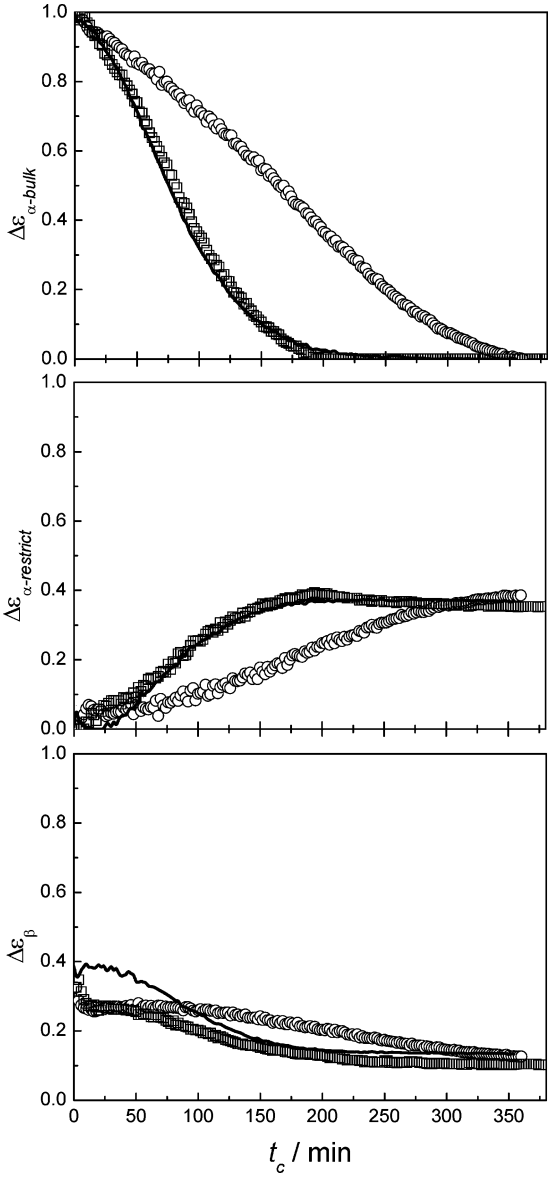

Figure 3. Evolution of the dielectric strength of $PLLA_{269kD}$ during cold crystallization (squares) and melt crystallization (circles) of the three relaxations detected: top graphics, α-relaxation for the nearly amorphous phase (α_{NA}); middle graphics, α-relaxation for the semicrystalline phase (α_{SC}); bottom graphics, β-relaxation. Results for a lower molecular weight PLLA, $PLLA_{86kD}$, during cold crystallization were included as solids lines for comparison. Dielectric strength values were normalized by the maximum value obtained for the nearly amorphous α-process.

spectra were collected as previously for 6 h. Figure 2b presents the experimental loss curves and respective fittings as solid lines; the inset shows the real and imaginary parts of the complex permittivity collected at 160 min, where solid lines are the corresponding overall fittings obtained by using the same individual HN functions also depicted.

Once again, data were able to be fitted as a sum of exactly the three same HN functions used in cold crystallization, having only different dielectric strengths. The main reason for intensity changes concerns to thickness differences since after melting the sample gets thinner.

Figure 3 includes the variation of the normalized dielectric strength thus obtained (circles). There is a less abrupt decay of the relaxation strength for the bulklike glass transition relaxation process only vanishing for $t_c = 350$ min, i.e., 150 min later than for the cold crystallization process. The same happens with the emerging of the constrained α-process; i.e., the respective dielectric strength increases more gradually during melt crystallization, meaning that this crystallization process develops slower relative to cold crystallization. This is not surprising since the number of crystal nuclei that are produced during quenching should be considerable, as the nucleation rate increases with the distance to the equilibrium melting temperature. Therefore, during cold crystallization a greater number of spherulites will grow at a given crystallization temperature with respect to the crystallization at the same conditions with the material coming from the melt. Such difference in the spherulitic development can be observed by optical microscopy (see, for example, ref 17).

Also included in Figure 3 are the normalized dielectric strength values for $PLLA_{86kD}$ obtained during crystallization at 80 °C after melting at 200 °C (solid lines), thus corresponding to a melt crystallization process. This plot allows evaluating the influence of molecular weight, where the solid lines, for $PLLA_{86kD}$, should be compared with the circle symbols (higher molecular weight $PLLA_{269kD}$ studied in this work), evidencing how the molecular weight decrease accelerates the crystallization progress. Although the general trends are similar, the evolution of the crystallization process, as monitored through the changes occurring within the amorphous fraction, is much faster for $PLLA_{86kD}$. Such a difference was already observed during nonisothermal cold crystallization of the same two polymers, observed by simultaneous SAXS and WAXS and DSC:[28] it was shown that the crystallization rate of PLLA decreases with increase of molecular weight.

Figures 2 and 3 demonstrate that the assumptions used to treat dielectric data are valid for two different molecular weights and are independent whenever we consider cold or melt crystallization. This provides new support to state that, at least for PLLA, the development of crystallinity leads to the formation of a more restricted amorphous phase, which increases in magnitude during crystallization, with a concomitant vanishing of the initial bulklike amorphous phase. This process seems to occur since the very initial stages of crystalline evolution; i.e., the effect of lamellar confinement in the amorphous phase is observed as the total dielectric strength of the loss modulus is decreasing. In fact, Figure 3 shows an increase of $\Delta\epsilon_{\alpha_{SC}}$ in the very initial stages of the crystallization, when a decrease in $\Delta\epsilon_{\alpha_{NA}}$ is also observed. We hypothesize that the origin of the α_{SC} relaxation should be a result of the confined mobile amorphous phase placed between the crystalline lamellae, which start to be formed in the primary crystallization step. Besides the mobile amorphous phase, there is also the formation of a rigid amorphous phase placed between the mobile amorphous layer and the crystalline lamellae.[29] The concept of rigid amorphous phase was introduced to elucidate the discrepancies between the theoretical and experimental heat capacities at T_g, determined by DSC.[30,31] The appearance of this phase does not contribute for the increase of $\Delta\epsilon_{\alpha_{SC}}$, but contributes for the decrease of $\Delta\epsilon_{\alpha_{NA}}$, because no segmental motions take place in such regions. Therefore, the much more notorious decrease in $\Delta\epsilon_{\alpha_{NA}}$ is explained by the consumption of amorphous polymer with a bulklike behavior giving rise to crystalline material and rigid amorphous phase that occurs in a higher extent relative to the simultaneous buildup of a confined mobile amorphous phase, quantified by a lower increase of $\Delta\epsilon_{\alpha_{SC}}$. Cebe and co-workers showed that the content of the rigid amorphous phase should increase systematically with the crystallization time.[32]

The α_{SC} relaxation is broader than the α_{NA} process (the HN α parameter is 0.43 and 0.53, respectively). This is consistent

with the general observation that the loss peak of the α-relaxation for semicrystalline polymers is broader than for the corresponding amorphous material[16] and is also consistent with previous DSC results in PLLA.[33] When confined within the crystalline structure the mobile polymeric segments will experiment a wider variety of environments, as they can site more or less apart from the stiff walls, leading to a broadening of the distribution of relaxation times.

Some authors studying different polymers under isothermal crystallization opted to fit the global loss peaks by using a single HN function (see, for example, refs 34−36). In such cases a broadening was continuously observed since the very initial stages of crystallization, as perceived by a decrease in the α_{HN} parameter. Such observations strengths the suggestion that the influence of the confinement caused by the crystalline fraction starts to be effective during primary crystallization, i.e., the entrapped amorphous layer between the lamellae have a component (mobile amorphous region) with a slower dynamics characterized by a broader distribution of relaxation times, as compared with the bulklike α-relaxation. During isothermal crystallization it was seen, from small-angle X-ray scattering, that the thickness of the amorphous layer is kept approximately constant, around 5 nm.[37] Therefore, one should not expect a notorious variation of the features of the long-range segmental dynamics of the confined amorphous layer during isothermal crystallization, i.e., the component of the global loss process related to the confined glass transition should maintain both the shape parameters and the position in the frequency axis. This information is implicit in the proposed model, where we suggest that the loss peak should be given by a linear combination of two "pure" loss processes. Therefore, the widening of the global loss peak observed during crystallization has two origins: the fact that the α_{SC} loss peak is intrinsically broader than the α_{NA} and the fact that at intermediate crystallization times we have the influence of both processes. We may even hypothesize that, if the difference of the position of the two relaxations was larger, we could have, with increasing t_c, a broadening of the global loss peak (due to the combination of both α_{NA} and α_{SC}) followed by a reduction in broadness, toward to the pure loss peak of the α_{SC} relaxation.

3.3. Semicrystalline State. After each crystallization process, the dielectric properties of $PLLA_{269kD}$ were measured from −120 up to +140 °C, in an enlarged frequency range to detect the crystallization influence in the secondary β-relaxation and to characterize the remaining α-restricted glass transition relaxation process.

Figure 4a presents the dielectric loss spectra obtained after completing cold crystallization from 25 up to 140 °C, where mainly the α_{SC} is observable. Nevertheless, the β-relaxation is felt in the high-frequency side as shown in the inset obtained at 80 °C, where the two individual HN functions used to obtain the overall fitting are depicted. The real part of the complex permittivity is also shown (open circles) where the solid line represents the HN fitting using the same two individual functions. The isochronal plot at 1 kHz taken from isothermal measurements is shown in Figure 4b in logarithmic scale, relative to data collected after melt crystallization, evidencing both β- and α_{SC}-relaxation processes.

Both β- and α_{SC}-processes were fitted with the Havriliak−Negami equation; an additional term, $i(\sigma/\omega\epsilon_0)$, was added for fitting dielectric loss at temperatures higher than 80 °C, to take into account dc conductivity (σ). The resulting shape parameters and dielectric strength are presented in Figure 5a for the β-process and Figure 5b for the α_{SC}-relaxation process.

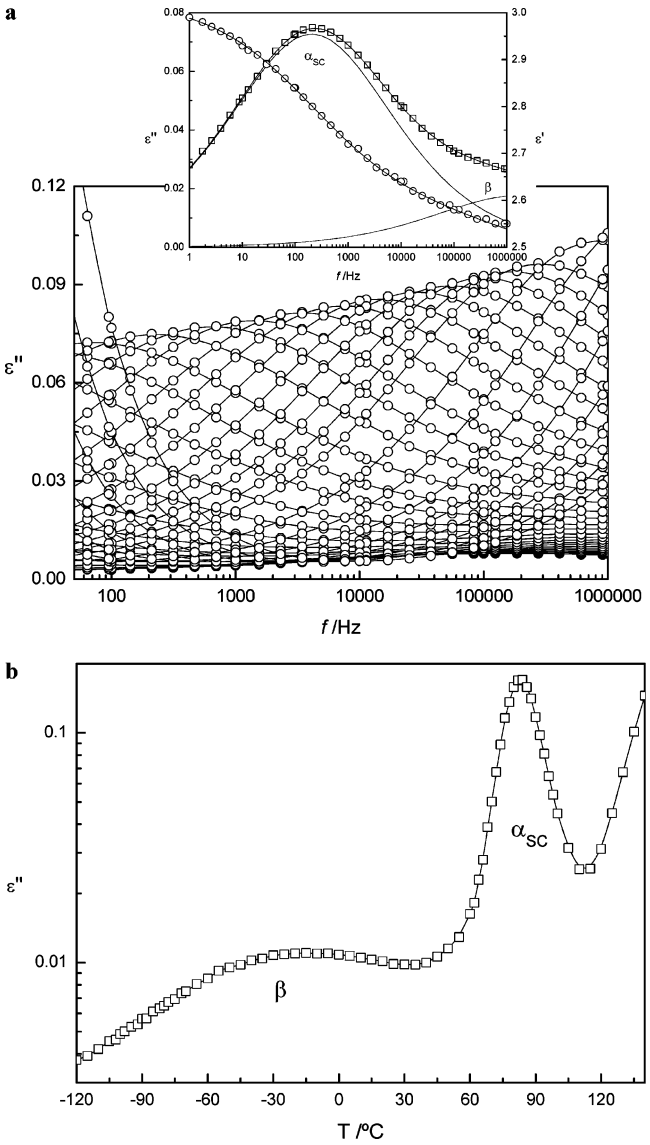

Figure 4. (a) Isothermal dielectric loss spectra for the constrained α-process detected after cold crystallization of $PLLA_{269kD}$ within the temperature range from 25 to 140 °C. The inset shows the imaginary (squares) and real (circles) parts of the complex permittivity at 80 °C where the solid lines represent the overall fitting by taking in account two individual HN functions (α_{SC} and β) also depicted. (b) Dielectric loss in logarithmic scale at 1 kHz taken from the isothermal measurements in function of temperature covering full range for the constrained α-process detected after melt crystallization of $PLLA_{269kD}$ at 80 °C.

The dielectric strength for the β-relaxation (squares in Figure 5a) shows a small increase with the temperature increase as usually happens for a secondary relaxation with a slight increase of the α_{HN} shape parameter (circles in Figure 5a): full symbols for secondary process detected after cold crystallization and open symbols for process detected after melt crystallization. The β_{HN} shape parameter was found to be 0.79 ± 0.03 for the secondary relaxation detected, being equal to the value found for the relaxation detected in the amorphous state.

In what concerns the constrained α-process (Figure 5b), the dielectric strength (squares) slightly decreases with increasing temperature for this process detected either after cold (full symbols) or melt (open symbols) crystallizations. The respective α_{HN} shape parameters (circles) increase with the temperature increase, revealing the narrowness of the distribution of relaxation times with simultaneous symmetry increase ($\beta_{HN} = 1$).

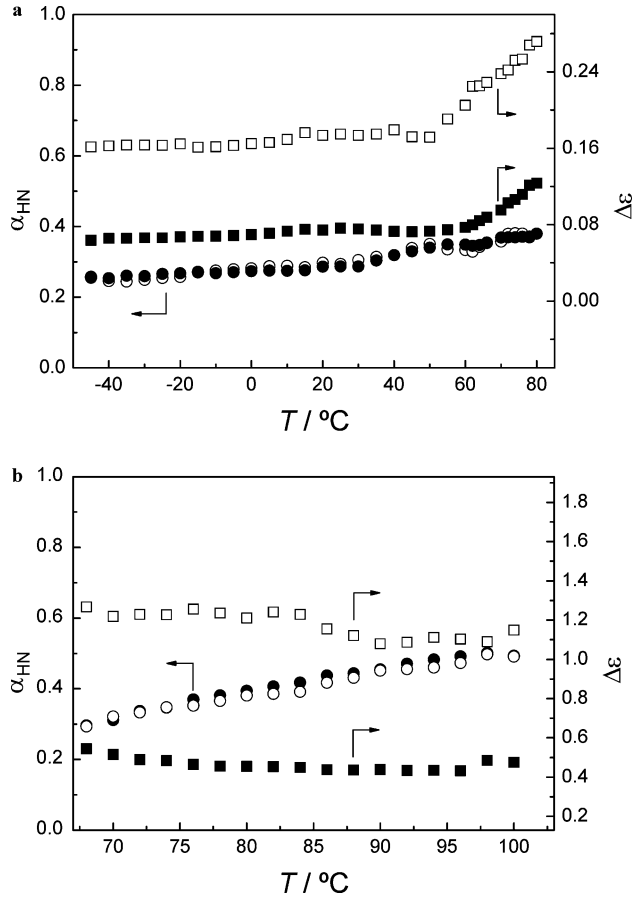

Figure 5. Temperature dependence of α_{HN} shape parameter (circles) and dielectric strength, $\Delta\epsilon$ (squares), estimated through fitting for (a) β-relaxation and (b) constrained α-process detected after cold (full symbols) and melt (open symbols) crystallizations of $PLLA_{269kD}$.

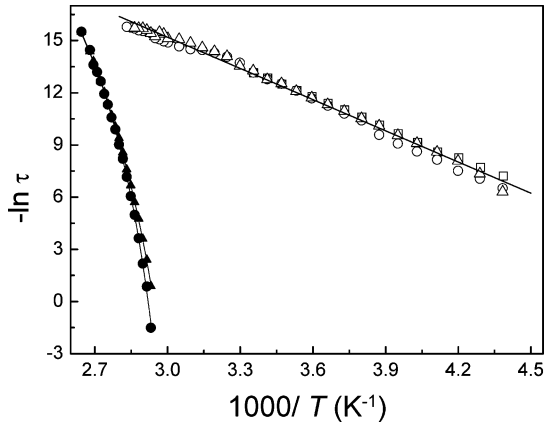

Figure 6. Relaxation map for all the relaxation processes detected in $PLLA_{269kD}$: the secondary process (open symbols), the α-constrained relaxation (full symbols) detected after cold crystallization (circles) and after melt crystallization (triangles); the temperature dependence for the β-relaxation detected in the amorphous sample prior to crystallization is also included (squares). The relaxation times are in seconds.

The temperature dependence of the obtained relaxation times is shown in Figure 6 for all processes detected.

As a first observation the secondary relaxation process (open symbols) shows the expected arrhenian dependence while the α-constrained relaxation process (full symbols) exhibits the usual curvature of cooperative processes.

Second, there are no significant differences relative to the crystallization method (circles, after cold crystallization; triangles, after melt crystallization) for both relaxation processes.

Additionally, in what concerns the β-process, a superposition with the equivalent process detected in the amorphous state (squares) is observed; thus, the mobility of this secondary process is not affected by crystallization. The effect of crystallinity in the β-relaxation has been analyzed before. Typically, for flexible polymers, the features of this process are not sensitive to the presence of crystallinity.[38] However, for more stiff materials, a different behavior can be found. For example, for poly(ether ether ketone) it was seen that the isochronal loss maxima of crystallized material were shifted toward higher temperatures as compared with the amorphous polymer, indicating that the extent of the motions assigned to this secondary process is greater than would be expected for typically subglass relaxations.[39] From the PLLA we may conclude that the dipole fluctuations assigned to the β-relaxation cover volumes that should be substantially smaller than the geometrical confinement imposed by the crystalline structures, developed from both cold and melt crystallization.

From the three linear dependences of the β-process a mean activation energy of 50 ± 3 kJ mol^{-1} was estimated. This value is higher than the activation energy of 36 kJ mol^{-1} found by other authors for PLLA,[40,41] being also superior to the values in the range 36−46 kJ mol^{-1} found for a series of L-lactide/meso-lactide copolymers.[22]

In what concerns the temperature dependence of both α-constrained relaxation processes, data were fitted by the Vogel−Fulcher−Tamman[42] equation (solid lines in Figure 6):

$$\tau = \tau_0 e^{B/T-T_0} \qquad (3)$$

with the following parameters: α_{SC} after cold crystallization, $\tau_0 = (0.8 \pm 0.8) \times 10^{-15}$ s, $B = 1029 \pm 64$ K, and $T_0 = 308 \pm 1$ K; α_{SC} after melt crystallization, $\tau_0 = (1.0 \pm 0.8) \times 10^{-15}$ s, $B = 1631 \pm 76$ K, and $T_0 = 292 \pm 1$ K. Considering that the temperature obtained by replacing τ in eq 2 by 100 s is a good estimate of the glass transition temperature,[43] the so-obtained values are 338 and 334 K for the α_{SC} after respectively cold and melt crystallizations. Complementary DSC experiments performed in $PLLA_{269kD}$ crystallized at 80 °C from the glassy and melt states were performed, and the calorimetric T_g were found to be 343.0 and 342.3 K, respectively; the small difference although having the same trend does not allow confirming dielectric estimations, as the difference is not significant.

4. Conclusions

Isothermal cystallization of PLLA, coming from both the glassy or melt states, was monitored by DRS. During crystallization a shift of the main loss peak to lower frequencies around 1 decade is observed. Such behavior is general for both crystallization types and different molecular weights.

Loss data during crystallization are able to be fitted by a linear combination of three loss peaks: (i) the β secondary process at high frequencies, (ii) the α_{NA} process, observed for nearly amorphous material, and (iii) the loss peak for the fully transformed material (α_{SC}). The shape parameters and relaxation time are thus invariant during crystallizations and were also found to be essentially independent of both molecular weight and thermal history that anticipates crystallization, providing that crystallization is promoted at the same temperature.

The invariance of shape and relaxation time of the two α-relaxation processes indicate that their respective segmental dynamics develop independently and the dynamics features of the (slower) confined amorphous phase do not change during crystallization. The appearance of a clear contribution of α_{SC}

in the initial stages of crystallinity development suggests that the confinement effect of the lamellae takes place during primary crystallization. The $\Delta\epsilon$ evolution upon crystallization is slower for crystallization anticipated by melting and, for the same crystallization procedure, is retarded when M_w increases.

The secondary β-relaxation remains invariant after either crystallization type relative to the amorphous state, showing that the main dynamics features of this process are not influenced by crystallization.

Acknowledgment. Financial support for this work was provided by Fundação para a Ciência e Tecnologia, through the POCTI and FEDER programms and POCTI/FIS/61621/2004. M.T.V. and A.R.E.B. also thank Fundação para a Ciência e Tecnologia, for the Ph.D. Grants SFRH/BD/6661/2001 and SFRH/BD/23829/2005.

References and Notes

(1) Thomson, R. C.; Wake, M. C.; Yaszemski, M. J.; Mikos, A. G. *Adv. Polym. Sci.* **1995**, *122*, 245.
(2) Ikada, Y.; Tsuji, H. *Macromol. Rapid Commun.* **2000**, *21*, 117.
(3) Södegard, A.; Stolt, M. *Prog. Polym. Sci.* **2002**, *27*, 1123.
(4) Kim, H. D.; Bae, E. H.; Kwon, I. C.; Pal, R. R.; Nam, J. D.; Lee, D. S. *Biomaterials* **2004**, *25*, 2319.
(5) Miyata, T.; Masuko, T. *Polymer* **1998**, *39*, 5515.
(6) Di Lorenzo, M. L. *Polymer* **2001**, *42*, 9441.
(7) Sánchez, F. H.; Mateo, J. M.; Colomer, F. J. R.; Sánchez, M. S.; Ribelles, J. L. G.; Mano, J. F. *Biomacromolecules* **2005**, *6*, 3283.
(8) Yamashita, K.; Kikkawa, Y.; Kurokawa, Y.; Doi, Y. *Biomacromolecules* **2005**, *6*, 850.
(9) Renouf-Glauser, A. C.; Rose, J.; Farrar, D. F.; Cameron, R. E. *Biomaterials* **2005**, *26*, 5771.
(10) Salgado, A.; Wang, Y.; Mano, J. F.; Reis, R. L. *Mater. Sci. Forum* **2006**, *514*−*516*, 1020.
(11) Wang, Y.; Mano, J. F. *J. Appl. Polym. Sci.* **2006**, *100*, 2628.
(12) Ivanov, D. A.; Pop, T.; Yoon, D. Y.; Jonas, A. M. *Macromolecules* **2002**, *35*, 9813.
(13) Forrest, J. A.; Danolki Veress, K. *Adv. Colloid Interface Sci.* **2001**, *94*, 167.
(14) Schönhals, A.; Goering, H.; Schick, Ch.; Frick, B.; Zorn, R. *J. Non-Cryst. Solids* **2005**, *351*, 2668.
(15) Ngai, K. L.; Roland, C. M. *Macromolecules* **1993**, *26*, 2688.
(16) Kremer, F., Schönhals, A., Eds.; *Broadband Dielectric Spectroscopy*; Springer: Berlin, 2002.
(17) Mijović, J.; Sy, J. W. *Macromolecules* **2002**, *35*, 6370.
(18) Fitz, B. D.; Andjelić, S. *Polymer* **2003**, *44*, 3031.
(19) Dionísio, M.; Viciosa, M. T.; Wang, Y.; Mano, J. F. *Macromol. Rapid Commun.* **2005**, *26*, 1423.
(20) Lee, B.; Shin, T. J.; Lee, S. W.; Yoon, J.; Kim, J.; Ree, M. *Macromolecules* **2004**, *37*, 4174.
(21) Wang, Y.; Ribelles, J. L. G.; Sánchez, M. S.; Mano, J. F. *Macromolecules* **2005**, *38*, 4712.
(22) Kanchanasopa, M.; Runt, J. *Macromolecules* **2004**, *37*, 863.
(23) Havriliak, S.; Negami, S. *Polymer* **1967**, *8*, 161.
(24) Ren, J.; Urakawa, O.; Adachi, K. *Macromolecules* **2003**, *36*, 210.
(25) Arndt, M.; Stannarius, R.; Groothues, H.; Hempel, E.; Kremer, F. *Phys. Rev. Lett.* **1997**, *79*, 2077.
(26) McKenna, G. B. *J. Phys. IV* **2000**, *10 Pr7*, 53.
(27) Wang, Y.; Funari, S. S.; Mano, J. F. *Macromol. Chem. Phys.* **2006**, *207*, 1262.
(28) Mano, J. F.; Wang, Y.; Viana, J. C.; Denchev, Z.; Oliveira, M. J. *Macromol. Mater. Eng.* **2004**, *289*, 910.
(29) Iannace, S.; Nicolais, L. *J. Appl. Polym. Sci.* **1997**, *64*, 911.
(30) Cheng, S. Z. D.; Wunderlich, B. *Macromolecules* **1988**, *21*, 789.
(31) Wunderlich, B. *Prog. Polym. Sci.* **2003**, *28*, 383.
(32) Xu, H.; Ince, B. S.; Cebe, P. *J. Polym. Sci., Part B: Polym. Phys.* **2003**, *41*, 3026.
(33) Mano, J. F.; Gómez Ribelles, J. L.; Alves, N. M.; Salmerón, M. *Polymer* **2005**, *46*, 8258.
(34) Natesan, B.; Xu, H.; Ince, B. S.; Cebe, P. *J. Polym. Sci., Part B*: *Polym. Phys.* **2004**, *42*, 777.
(35) Laredo, E.; Grimau, M.; Barriola, P.; Bello, A.; Müller, A. J. *Polymer* **2005**, *46*, 6532.
(36) Sanz, A.; Nogales, A.; Ezquerra, T. A.; Lotti, N.; Munari, A.; Funari, S. S. *Polymer* **2006**, *47*, 1281.
(37) Cho, J.; Baratian, S.; Kim, J.; Yeh, F.; Hsiao, B. S.; Runt, J. *Polymer* **2003**, *44*, 711.
(38) Boyd, R. H. *Polymer* **1985**, *26*, 323.
(39) Kalika, D. S.; Krishnaswamy, R. K. *Macromolecules* **1993**, *26*, 4252.
(40) Starkweather, H. W.; Avakian, P.; Fontanella, J. J.; Wintersgill, M. C. *Macromolecules* **1993**, *26*, 5084.
(41) Henry, F.; Costa, L. C.; Devassine, M. *Eur. Polym. J.* **2005**, *41*, 2122.
(42) Vogel, H. *Phys. Z.* **1921**, *22*, 645. Fulcher, G. S. *J. Am. Chem. Soc.* **1925**, *8*, 339. Tammann, G.; Hesse, W. *Z. Anorg. Allg. Chem.* **1926**, *156*, 245.
(43) *Disorder Effects on Relaxational Processes*; Richert, R., Blumen, A., Eds.; Springer: Berlin, 1994.

MA061148R